

Malaria Early Warning Application for Individual Risk Assessment

Sagar Sadak¹, Cayden Goeringer², and Janiah Kyle³

Project Advisor: Abba Gumel⁴

Abstract As one of the oldest known diseases to inflict humanity (since the Agricultural Revolution about 12,000 years ago), malaria has proven to be a significant global challenge. Many intervention strategies have been undertaken in the last few decades such as widespread insecticide-treated bed nets (ITN), long-lasting insecticidal nets (LLIN) and indoor residual spraying (IRS). Yet even with great success, malaria continues to be a ravaging disease requiring inventive solutions. In this study, we develop a malaria early warning system, which utilizes an adapted Ross-MacDonald model to assess individual risk and disease epidemiology. Strategies for achieving a disease-free equilibrium state are also shown by performing local asymptotic stability analysis. It is important to note that the stages of the mosquito life-cycle are highly influenced by weather conditions, both in the aquatic and adult stages, as well as by the use of insecticides (either through ITN/LLIN use or via IRS). Therefore, we consider regional data parameters, such as weather conditions, parasite rate and resistance, to estimate deviated risk from the baseline, with the final product being a progressive web application (i.e. a web and mobile app). Such a product has widespread application primarily in holoendemic areas in Africa to inform both native and tourist populations of their relative risk of contracting malaria.

1. Introduction

Malaria is mainly a tropical disease caused by the parasitic *Plasmodium*, transmitted via the bite of infected female *Anopheles* mosquitoes. *Plasmodium* are a species of sexually-reproducing eukaryotic protozoans, whose life-cycle involves the affliction of two hosts - an invertebrate host (e.g. mosquitoes) that serves as a vector for transmission and a site for sexual reproduction, and a vertebrate host (e.g., reptiles, rodents, primates) where asexual reproduction and sexual development occurs, leading to the disease we know as malaria [1].

¹College of Computing, Georgia Institute of Technology, Atlanta, Georgia, USA. [sadaksagar9@gmail.com]

²School of Life Sciences, Arizona State University, Tempe, Arizona, USA. [caydengoeringer@gmail.com]

³Spelman College, Atlanta, Georgia, USA. [janiah.kyle@gmail.com]

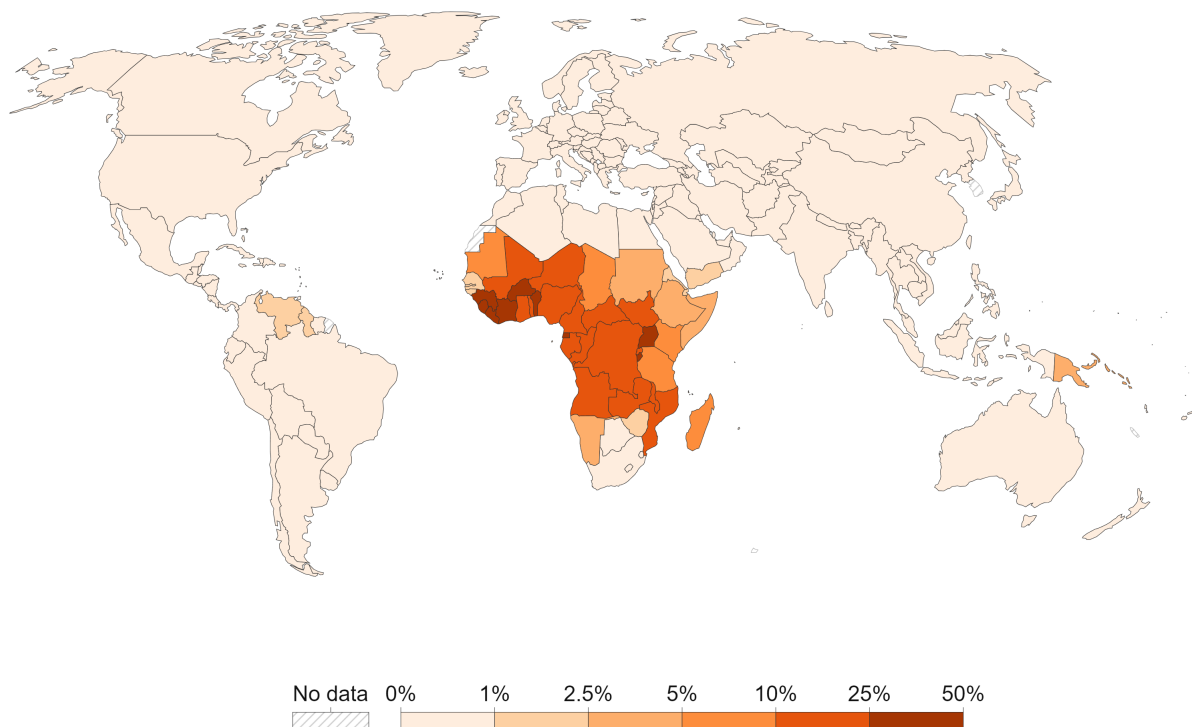
⁴Department of Mathematics, University of Maryland, College Park, MD, USA. [agumel@umd.edu]

Of the five species of *Plasmodium* that affect humans, two are most notable: *P. falciparum* and *P. vivax*. Since *P. falciparum* is most prevalent in sub-Saharan Africa, it is the primary focus of this study.

Now consider the life cycle of an Anopheles mosquito. Both the immature and adult stages are highly dependent on weather conditions such as temperature and precipitation. Mosquitoes favor relatively warm tropical climates, stagnant water bodies, and a sufficient population of hosts to acquire a blood meal (for the egg development process). Compounding to these factors that mosquitoes prefer are the broader socioeconomic background of residents, land-use practices, and the level of development of the area (including sanitation infrastructure and the availability of medical care). All of these affect the prevalence level of malaria and, subsequently, its risk of contraction for any particular location. As illustrated in Figure 1, the areas that meet these criteria tend to have a larger percentage of the population at risk. This idea is the backbone of our application; local variability is used to assess risk in relation to the annual baseline.

Share of the population with malaria, 2019

Our World
in Data



Source: IHME, Global Burden of Disease (2019)

OurWorldInData.org/malaria • CC BY

Figure 1. Percentage of population at risk of malaria in 2019. As shown, most of the risk is concentrated in Africa and certain countries in southeast Asia and South America. Source of figure: [2].

With nearly half the world's population at risk of this disease, its eradication has been of primary concern to various organizations around the world, such as the World Health Organization (WHO), the Bill and Melinda Gates Foundation, and the US President's Malaria Initiative [3]. Although significant steps have been taken towards its eradication by a multitude of such groups, it is nevertheless a leading cause of death in many developing countries. Although it is preventable and curable, it was responsible for 241 million cases and 627,000 deaths in 2020 alone [3]. The continent of Africa, specifically the western and central regions, are most affected by this disease, accounting for around 95% of the cases and 96% of the deaths, with a vast majority of these deaths (~80%) occurring in children under the age of 5 [3]. The socioeconomic development of many countries is greatly afflicted by malaria. The disease has been proven, since as early as 1965, to cause much lower economic growth; reductions in malaria are associated with much higher economic growth [4]. Thus, malaria warrants immediate global cooperative action [5].

A key tool in malaria prevention has been the insecticide-treated bed nets (ITNs) and long-lasting insecticidal nets (LLINs) with their great success evident by the distribution of 2 billion nets to sub-Saharan Africa between 2004-2020 [3]. The use of ITNs has proven to be useful for prevention and even reduction of childhood mortality [6]. In recent years, however, growing resistance of the mosquitoes to insecticides has rendered many pyrethroid chemicals (and thus, ITNs and LLINs) less effective [7]. Across nearly all of Africa, resistance has been observed to some extent and even across different vector groups due to many different evolved mechanisms including knockdown resistance [8].

Since ITNs and LLINs alone are not sufficient for eradicating malaria, a combination of preventive measures is currently the best course of action. Therefore, we developed a malaria early warning system (MEWS) as a mobile application and website to warn users of their risk of contracting malaria in a specific region. The goal is that it serves as a site for the spread of reliable, life-saving information regarding malaria, as well as to inspire behavioral changes in people whether it be through advising the use of bed nets or to stay away from stagnant water bodies servicing as mosquito breeding spots. The MEWS will be an important component in the fight against malaria as it provides real-time information to the general public about potential risk in order to prevent additional cases.

Previous works for a malaria early warning system (MEWS) have had similar, but not identical, ideas and methods. One online MEWS recognizes the effects rainfall has on transmission and focuses on creating an early warning system for rain so the user can then predict the risk of contracting malaria [9]. However, the risk itself is not calculated, or at least not blatantly stated, by the system itself. In addition, most of the graphs presented focus only on rainfall and require interpretation from the user, making the experience less user-friendly than our MEWS. Another online MEWS provides more detailed information: Vulnerability, Seasonal Climate Forecasts, Monitoring the Environment and Observed Malaria Morbidity, but can only be used in English, French, and

Spanish, and does not offer any major African languages [10]. Moreover, it can only be accessed as a website, not a mobile application, and demands some background knowledge from the user. The website is furthermore ill-designed and hard to navigate, and similar to the previous MEWS, it does not calculate the risk and present it to the user. There exists an MEWS as a mobile application, but it is intended to be used by health workers for malaria reporting, case management, and surveillance in the Greater Mekong Subregion, including Myanmar [11]. It is not designed for the general public to use across many regions, unlike our MEWS. The novelty in our MEWS is that it is accessible through the web or as a mobile application and is user-friendly, in that it aims to penetrate to a larger user base, by not requiring any background knowledge from the user to interpret the risk result shown. In addition to English, our MEWS also includes the most common African languages: French, Swahili, Yoruba, and Igbo so those who are at higher risk of contracting the disease can use the application.

Our MEWS will first obtain the user's current location or the location he/she will travel to in the future, then obtain the relevant data, such as temperature and parasite rate, to evaluate potential infections and the user's individual risk. For this, the MEWS requires mathematical modeling that can be evaluated at any given time. Thus, our mathematical model consists mostly of differential equations, forming a compartmental model.

The rest of the paper expands on the mathematical model used, the mathematical logic behind it, as well as the application itself.

2. Mathematical Models

The model used in this study has a long history traced back to the first models of malaria from Sir Ronald Ross in the early 1900s. His work was advanced in the following decades by those such as Alfred J. Lotka and George Macdonald to more accurately capture the disease's properties [12]. From the progression of these mathematical models came new ideas including entomological inoculation rate, basic reproduction number, and vectorial capacity which addressed the need to assess transmission and epidemiology [12]. More recent advancements have improved the accuracy of past models by including properties related to immunity and climate. The epidemiology of malaria since Macdonald has also highlighted the importance of endemicity when observing populations with the disease. Requirements to meet potential eradication have been implemented but ultimately failed [12].

Another crucial component of modeling malaria is considering the role of weather on mosquito population dynamics. The early work of Lysenko and Semashko made initial discoveries of the temperatures required to sustain transmission and was thus influential for malarial endemicity, highlighting malaria global maximums nearer to the equator [13][14]. Although other weather factors such as rainfall and humidity contribute to malaria abundance, the role of temperature is especially important given that *Plasmodium falciparum* can maintain growth cycles until temperatures drop below 20°C [15].

Using real-time weather data, insecticide resistance data, malaria prevalence, and bed net usage data, we generated solutions to our model equations numerically using the *odeint* command from the *scipy* library method in Python (Version 3.10.1). What we get is the entomological inoculation rate (EIR), which is used to inform the user of his/her relative risk at his/her location. This is the basic premise of the MEWS progressive web application that we develop as part of this study.

In order to calculate the risk of contracting malaria in a particular region, dynamic mathematical models must be developed for both humans and mosquitoes. The human model and mosquito model are SEIR and SEI models respectively. For the mosquito dynamics, it is important to include both the adult stage and the immature/aquatic stage since both stages depend on one another. Only adult mosquitoes bite for blood meals, thus only adult mosquito dynamics are an SEI model. The immature mosquitoes will determine how many adult mosquitoes there will be. Therefore, the immature dynamics are an important factor in analyzing malaria transmission. Since humans have the ability to recover from malaria, the human dynamics are an SEIR model. Both the entomological inoculation rate (EIR) and the reproduction number of the disease (R_0) are helpful in determining the risk of contracting malaria. However, this paper only considers EIR.

2.1 Immature/Aquatic Mosquito Dynamics

The mosquito immature/aquatic stage is comprised of six classes: the egg class, four larva classes, and the pupa class. Mosquitoes are first born as eggs on a body of water. After they hatch, they are considered larvae, which go through four stages of development. After going through all the larva stages, they become pupae and then finally grow into adult mosquitoes.

For simplicity, this model combines all four larva classes into one class, thus having a total of three differential equations to represent the immature/aquatic stage of mosquitoes. Figure 2 illustrates the immature/aquatic stage dynamics.

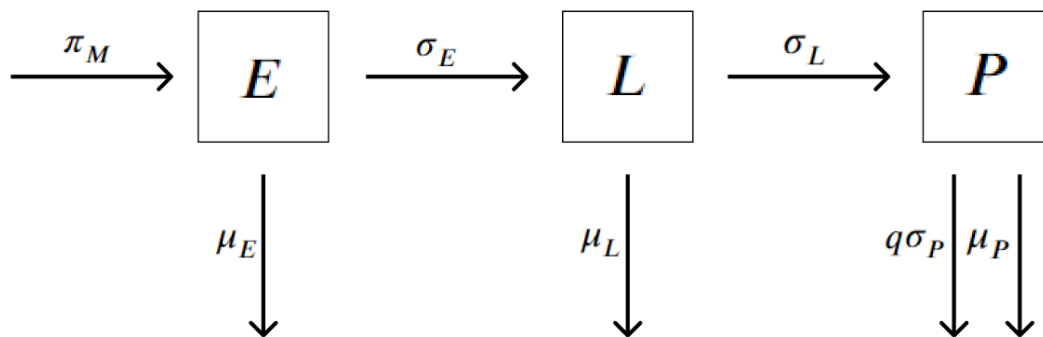


Figure 2. A graphic flowchart that illustrates the immature/aquatic stage dynamic model. The π_M term substitutes $\eta_E(T) \left(1 - \frac{E}{K_E}\right) (N_m)$.

The variables E , L , and P are the number of eggs, larvae, and pupae respectively. In the figure above, π_M is a substitute variable that represents the expression $\eta_E(T) \left(1 - \frac{E}{K_E}\right) (N_m)$. The parameter $\eta_E(T)$ is the number of eggs laid per adult female mosquito per day [16]. This parameter is a temperature dependent function and its details can be found in Table 4, along with a graphical visualization in Figure 6. To obtain the remaining proportion of potential eggs that can be laid in the future, the proportion of current eggs, E , to egg carrying capacity, $K_E(R)$, is subtracted from 1. Note that the carrying capacity, K_E , as a function is dependent on rainfall (R). An in-depth mathematical explanation for how rainfall is accounted for in the MEWS is provided later in the paper, in the app section. The total number of adult female mosquitoes, N_m , is then multiplied by the product of the number eggs laid per female mosquito per day, $\eta_E(T)$, and the proportion of potential eggs that can be laid in the future, $\left(1 - \frac{E}{K_E(R)}\right)$. It is necessary to subtract eggs that develop into larva or die from this expression (See Table 2 for the descriptions of each parameter). The larva class receives immature mosquitoes that survived the egg class and loses larva that either progress to the pupa class or die off. The pupa class goes through a similar process with consideration that the proportion that are female, q , are the only type of mosquitoes we want to observe for the adult class. Thus, the differential equations derived from Figure 2 (where a dot represents differentiation with respect to time t) are below:

$$\dot{E} = \eta_E(T) \left(1 - \frac{E}{K_E(R)}\right) N_m - \sigma_E(T)E - \mu_E(T)E,$$

$$\dot{L} = \sigma_E(T)E - \sigma_L(T)L - \mu_L(T)L,$$

$$\dot{P} = \sigma_L(T)L - q\sigma_P(T)P - \mu_P(T)P.$$

The formula for carrying capacity is adapted from White et al., which was modeled as a convolution of recent rainfall with some weighting function which had been included as either a constant, linearly decreasing, or exponentially decreasing function. The constant weighting function was used here for simplicity:

$$K(t) = \lambda \frac{1}{\tau} \int_{t-\tau}^t \text{rain}(t') dt',$$

where $\text{rain}(t)$ is daily rainfall and λ is the fitted scaling factor unique to the population data [17].

2.2 Adult Mosquito Dynamics (sensitive to insecticides)

After surviving the immature stage, female mosquitoes develop into adults, seek hosts for blood, and thus, are susceptible to malaria. A female mosquito that bites an infectious human moves from the susceptible class to the exposed class. A mosquito that becomes infectious at a rate σ_{ms}

moves from the exposed class to the infectious class. Mosquitoes that die at the natural death rate μ_{ms} or die from contact of insecticide treated bed nets (ITNs) at a rate $\epsilon_B C_B \delta_B$ leave every class. Figure 3 illustrates this sensitive adult mosquito dynamic.

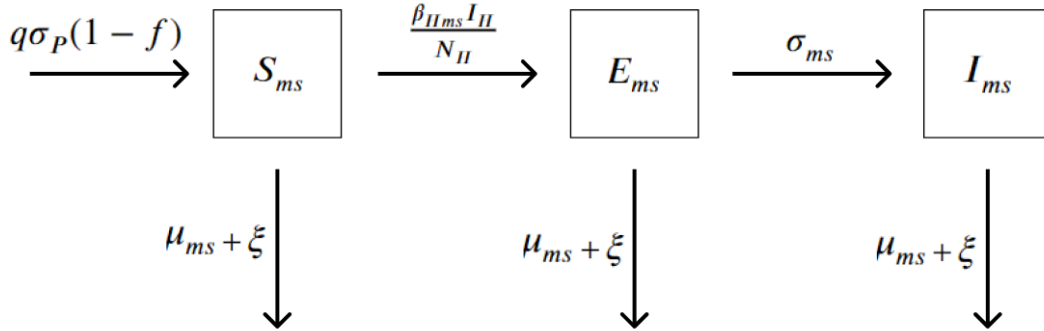


Figure 3. A graphic flowchart that illustrates the sensitive adult mosquito dynamic model. The ξ term substitutes $\epsilon_B C_B \delta_B$.

It is important to note that the expression $(1 - f)$ represents the proportion of female mosquitoes sensitive to an ITN compared to those resistant to insecticide. The differential equations derived from Figure 3 are as seen below:

$$\begin{aligned} \dot{S}_{ms} &= q\sigma_P(T)(1-f)P - \frac{\beta_{Hms} I_H S_{ms}}{N_H} - (\mu_{ms} + \epsilon_B C_B \delta_B) S_{ms}, \\ \dot{E}_{ms} &= \frac{\beta_{Hms} I_H S_{ms}}{N_H} - \sigma_{ms} E_{ms} - (\mu_{ms} + \epsilon_B C_B \delta_B) E_{ms}, \\ \dot{I}_{ms} &= \sigma_{ms} E_{ms} - (\mu_{ms} + \epsilon_B C_B \delta_B) I_{ms}. \end{aligned}$$

2.3 Adult Mosquito Dynamics (resistant to insecticides)

Similar to the adult mosquitoes sensitive to ITNs, Figure 4 illustrates the dynamics for the adult mosquitoes resistant to insecticide.

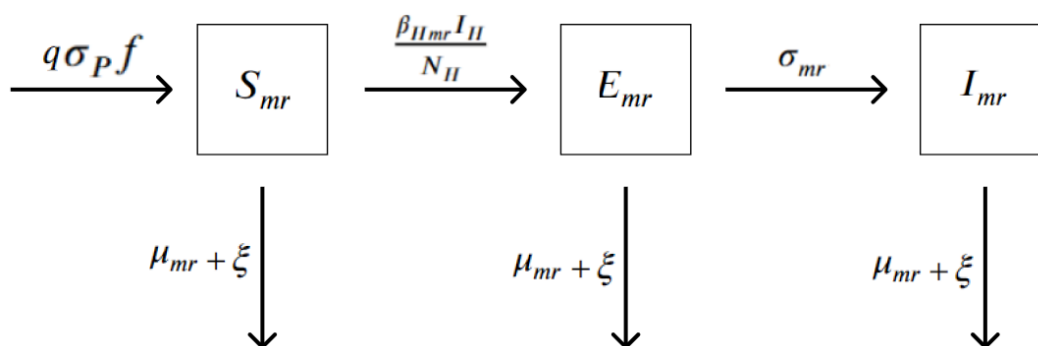


Figure 4. A graphic flowchart that illustrates the resistant adult mosquito dynamic model. The ξ term substitutes $\epsilon_B C_B \delta_B (1 - u)$.

Note that f is used instead of $(1 - f)$ to differentiate between resistant and sensitive mosquitoes, while the expression $(1 - u)$ is used to differentiate the killing rates due to insecticide (δ_B) [18]. The parameters σ_{ms} and σ_{mr} (rates for resistant/sensitive adult mosquitoes to become infectious) are temperature dependent functions. For simplicity, let the value of $\sigma_{ms} = \sigma_{mr} := \sigma_m$ (See Table 4). Therefore, the differential equations derived from Figure 4 are as seen below:

$$\begin{aligned} \dot{S}_{mr} &= q\sigma_P(T)fP - \frac{\beta_{Hmr}I_H S_{mr}}{N_H} - (\mu_{mr} + \epsilon_B C_B \delta_B (1 - u)) S_{mr}, \\ \dot{E}_{mr} &= \frac{\beta_{Hmr}I_H S_{mr}}{N_H} - \sigma_{mr} E_{mr} - (\mu_{mr} + \epsilon_B C_B \delta_B (1 - u)) E_{mr}, \\ \dot{I}_{mr} &= \sigma_{mr} E_{mr} - (\mu_{mr} + \epsilon_B C_B \delta_B (1 - u)) I_{mr}. \end{aligned}$$

2.4 Human Dynamics

In a region where malaria is prevalent, humans become susceptible as soon as they are born or when they migrate to that particular region. In the human dynamic model, this is the recruitment rate, π_H . A human bitten by an infectious mosquito (resistant or susceptible to insecticide) moves from the susceptible class to the exposed class. In the model below, bed net efficacy, ϵ_B , and bed net coverage, C_B , are considered to determine the probability of transmission when bed nets are being used. The human dynamic model is described in Figure 5 below.

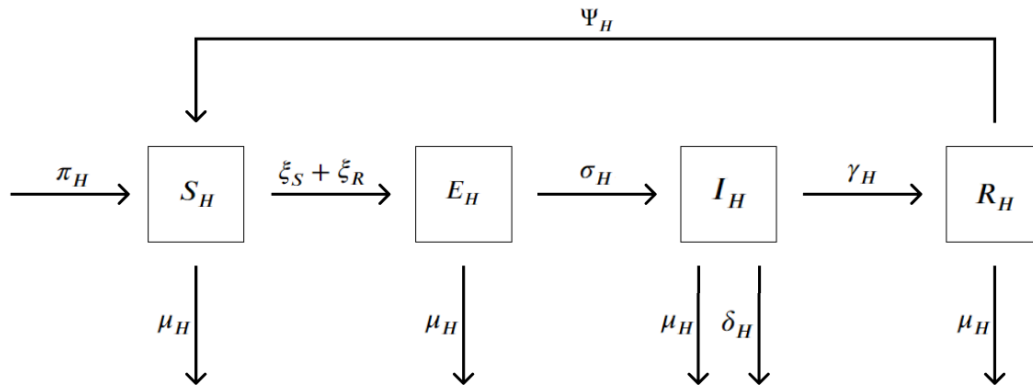


Figure 5. A graphic flowchart that illustrates the human dynamic model. The ξ_S and ξ_R terms substitute $(1 - \epsilon_B C_B) \left(\frac{\beta_{msH} I_{ms}}{N_H} \right)$ and $(1 - \epsilon_B C_B) \left(\frac{\beta_{mrH} I_{mr}}{N_H} \right)$, respectively.

Let μ_H be the natural death rate for humans and let σ_H be the rate at which humans become infectious. The parameter γ_H is the rate at which humans recover. Since immunity from malaria is only temporary, Ψ_H is the rate at which humans from the recovered class move back into the susceptible class. The differential equations derived from Figure 5 are as seen below:

$$\dot{S}_H = \pi_H - (1 - \epsilon_B C_B) \left(\frac{\beta_{msH} I_{ms}}{N_H} S_H + \frac{\beta_{mrH} I_{mr}}{N_H} S_H \right) - \mu_H S_H + \Psi_H R_H,$$

$$\dot{E}_H = (1 - \epsilon_B C_B) \left(\frac{\beta_{msH} I_{ms}}{N_H} S_H + \frac{\beta_{mrH} I_{mr}}{N_H} S_H \right) - \mu_H E_H - \sigma_H E_H,$$

$$\dot{I}_H = \sigma_H E_H - \gamma_H I_H - \mu_H I_H - \delta_H I_H,$$

$$\dot{R}_H = \gamma_H I_H - \mu_H R_H - \Psi_H R_H.$$

Malarial superinfection and waning immunity complicates the most accurate model representation of immunity, especially in holoendemic populations where complete susceptibility renewal rarely occurs. Dynamics of recurring infection have been considered in recent models [16].

Table 1. Description of State Variables

| Variables | Interpretation |
|-----------|---|
| E | Number of eggs |
| L | Number of larvae (combination of all 4 instar stages) |
| P | Number of pupae |
| S_{ms} | Number of susceptible mosquitoes that are sensitive to insecticides |
| E_{ms} | Number of exposed mosquitoes that are sensitive to insecticides |
| I_{ms} | Number of infectious mosquitoes that are sensitive to insecticides |
| S_{mr} | Number of susceptible mosquitoes that are resistant to insecticides |
| E_{mr} | Number of exposed mosquitoes that are resistant to insecticides |
| I_{mr} | Number of infectious mosquitoes that are resistant to insecticides |
| S_H | Number of susceptible humans |
| E_H | Number of exposed (infected but not infectious) humans |
| I_H | Number of infectious humans |
| R_H | Number of recovered humans |

Table 2. Description of Parameters

| Parameters | Interpretation |
|---------------------------|--|
| $\eta_E(T)$ | Eggs per female mosquito per day |
| $K_E(R)$ | Carrying capacity of eggs |
| q | Proportion of female mosquitoes |
| N_m | Total number of mosquitoes |
| $\sigma_E(T)$ | Development rate of eggs to larvae |
| $\mu_E(T)$ | Natural death rate of eggs |
| $\sigma_L(T)$ | Development rate of larvae to pupae |
| $\mu_L(T)$ | Natural death rate of larvae |
| $\sigma_P(T)$ | Development rate of pupae to adult |
| $\mu_P(T)$ | Natural death rate of pupae |
| f | Proportion of resistant mosquitoes |
| β_{HM} | Transmission probability from infected human to a susceptible mosquito |
| μ_{ms} | Natural death rate of susceptible mosquitoes that are sensitive to insecticides |
| ϵ_B | Efficacy of bed nets |
| C_B | Coverage of bed nets |
| δ_B | Bed net-induced mortality rate |
| σ_{ms} | Development rate of mosquitoes that are sensitive to insecticides from exposed to infectious |
| μ_{mr} | Natural death rate of susceptible mosquitoes that are resistant to insecticides |
| u | Decrease in mortality rate of resistant mosquitoes in comparison to sensitive mosquitoes |
| σ_{mr} | Development rate of mosquitoes that are resistant to insecticides from exposed to infectious |
| π_H | Recruitment rate of humans |
| β_{msH}/β_{mrH} | Transmission probability from infected mosquito (that is sensitive to insecticides/resistant to insecticides) to a susceptible human |
| β_{Hms}/β_{Hmr} | Transmission probability from infected human to a susceptible mosquito (that is sensitive to insecticides/resistant to insecticides) |

| | |
|------------|---|
| μ_H | Natural death rate of humans |
| Ψ_H | Rate of immunity loss of humans |
| σ_H | Development rate of humans from exposed to infectious class (Corresponds to time taken for <i>Plasmodium</i> to complete its schizogonic cycle) |
| γ_H | Recovery rate of humans from malaria |
| δ_H | Death rate of humans from malaria |
| N_H | Total number of humans |

Table 3. Values for Parameters

| Parameters | Baseline Values | Reference |
|------------|---|-----------|
| q | 0.5 (dimensionless) | [19] |
| f | 0.1 (dimensionless) | Assumed |
| u | 0.95 (dimensionless) | [20] |
| π_H | 2.19 (per day) | [20] |
| γ_H | 1/30 (per day) | [21] |
| Ψ_H | 0.0056 (per day) | [18] |
| σ_H | $\left(\frac{(12)(3.04)}{365}\right)$ (per day) | [16] |
| μ_H | 0.00004 (per day) | [16] |

Table 4. Functions for Dependent Parameters

| Parameters | Functions | Reference |
|----------------------|---|-----------|
| $\eta_E(T)$ | $\max(0, -0.153T^2 + 8.61T - 97.7)$ | [16] |
| $\sigma_{E,P}(T)$ | $\max(0, 6(-0.05 + 0.005T - 2.139 \times 10^{-16}e^T - 281357.656e^{-T}))$ | [21] |
| $\sigma_L(T)$ | $\max(0, \frac{6}{4}(-0.05 + 0.005T - 2.139 \times 10^{-16}e^T - 281357.656e^{-T}))$ | [21] |
| $\mu_{E,L,P}(T)$ | $8.929 \times 10^{-6}T^4 - 9.271 \times 10^{-4}T^3 + 3.536 \times 10^{-2}T^2 - 0.5814T + 3.509$ | [21] |
| $\beta_{Hms,Hmr}(T)$ | $\max(0, 0.022(-0.00014T^2 + 0.027T - 0.322))$ | [16] |
| $\beta_{msH,mrH}(T)$ | $\max(0, 0.24(-0.00014T^2 + 0.027T - 0.322))$ | [16] |
| σ_m | $\max(0, 0.000112T(T - 15.384)(\sqrt{35 - T}))$ | [21] |
| $\mu_{ms,mr}$ | $\left(\frac{1}{\max(0.1, -11.8239 + 3.3292T - 0.0771T^2)}\right)$ | [21] |

The high temperature dependency of the various parameters used in our model, as shown in Figure 6 below, serve as a crucial element in our MEWS. It can also be seen, as previously stated, how warmer tropical climates support the spread of malaria.

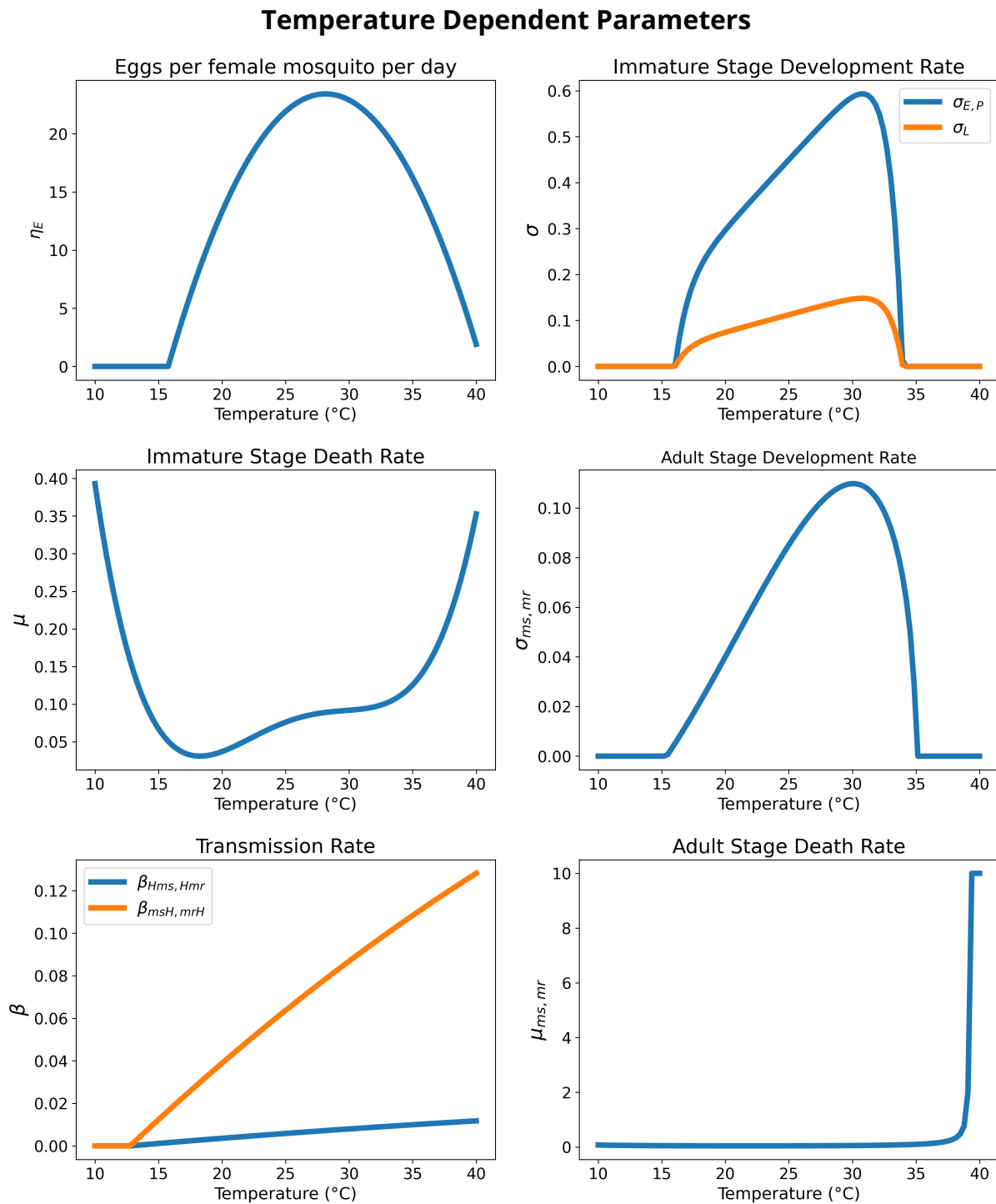


Figure 6. The figures above show the temperature-related dynamics of the model parameters, for which the equations are listed in Table 4.

2.5 EIR

The entomological inoculation rate (EIR) gives the rate of infectious bites per unit time (generally per day) per person. In the application, EIR is the main metric used to determine risk. The equation is described below:

$$EIR = \beta(1 - \epsilon_B c_B) \left(\frac{I_{ms} + I_{mr}}{N_H} \right).$$

The EIR is defined as the product of the rate of transmission (considering the effect of bed net usage) and the proportion of infectious mosquitoes to humans [16]. The proportion of infectious mosquitoes to humans is defined as the total number of infectious mosquitoes (both resistant and sensitive) over the total number of humans.

3. Progressive Web Application

There have been many advances in the multi-decade global effort to eradicate malaria. The use of bed nets, better living conditions, destruction of breeding sites, and more have proved to be effective in the decades past. However, insecticide resistance, among other issues, pose the next big obstacle to malaria eradication by 2040, one of United Nation's goals. Therefore, in response to these issues and as a culmination to this research paper, a web/mobile application has been developed using various technologies, including Python, JavaScript, HTML/CSS.

3.1 Data

Data is a major part of the app; acquiring and processing it posed one of the biggest issues during this study. To ensure a reliable risk approximation, we obtained data from multiple different sources, including locally saved datasets as well as APIs (Application Programming Interface). An in-depth explanation for each data point, including weather, insecticide resistance, malaria prevalence and mortality, and bed net usage, as well as their respective sources is provided below.

3.1.1 Weather

Temperature and precipitation have significant impacts on mosquito dynamics as many previous papers have studied [22][23]. Temperature affects nearly every single parameter in the aquatic and adult stages, whereas precipitation mainly influences the carrying capacity (K_E) of the eggs. This in turn has ripple effects that leads to changes in populations of mosquitoes as well as humans. The differential equations are solved using using the *odeint* command from the *scipy* library. Since the model is solved for a time range of 365 days before the present day, we used decadal monthly average temperature and precipitation data from WorldClim as an estimate for weather conditions

until 7 days before the present day. For the last week of the model solution, more accurate data is sourced from the WeatherAPI (Please note that accurate historical weather for more than one week can be accessed through the API with a paid subscription) [24][25].

The rainfall data is used to estimate rainwater accumulation in a specific region, in order to understand the existence of conditions favorable for the laying and development of mosquito eggs. Accumulation is calculated using the equation below, where τ represents the rate of loss of accumulated water (via evaporation or ground absorption). The value used for τ in our model is 7, signifying that it takes about 7 days, on average, for accumulated rainwater to disappear. This yields the following equation,

$$\dot{R} = \text{rain}(t) - \left(\frac{1}{\tau}\right) R.$$

The result is two arrays of length 365 consisting of temperature and rainwater accumulation data, respectively. As such, for each iteration of the model, these conditions are updated, and used to inform the parameter values, as described earlier in the paper.

3.1.2 Insecticide Resistance

The use of ITN/LLINs and IRS brought about huge success in combating malaria, vastly reducing the number of cases and deaths [3][26]. Unfortunately, however, this success turned out to be a double-edged sword. Alongside saving millions of lives, it also led to widespread resistance in mosquitoes, thus rendering the very tools that were effective a while ago, almost useless. This growing concern is one of the influences for this study and the development of this product. Until stronger insecticides are created or newer methods for fighting malaria are found, this app is expected to help ensure that populations, not only those local to Africa but also foreign tourists, are aware of the present risk of malaria in their respective regions.

3.1.3 Malaria Prevalence and Mortality

Knowing the demographic information for the user's location can allow us to accurately set the initial values for the state variables, i.e., S_H , I_H , etc. As such, a raster image is sourced from WorldPop, which consists of pixel-wise population data, with a resolution of 0.00833333 decimal degrees or approximately 1 kilometer [27].

This population data is coupled with the parasite rate raster image from the Malaria Atlas Project to, in turn, acquire the estimated number of infected humans (I_H) [28]. As expected, highly endemic areas will have higher parasite rates, thus leading to higher estimates of EIR. The Malaria Atlas Project is also the source of malaria-related human mortality data, corresponding to the parameter δ_H in our model.

3.1.4 Bed Net Usage

A present-day malaria model would not be an accurate representation of reality if it did not incorporate bed net usage and its effect on the mortality of mosquitoes for sensitive and resistant classes appropriately. The Malaria Atlas Project website hosts a research project that was conducted to gather this information, which was graciously made available for open access, enabling us to use it freely [28].

4. Results

4.1 Mathematical Proofs and Theorems

4.1.1 Basic Qualitative Properties

We monitor the temporal dynamics of mosquito populations using our mathematical model. All the state variables and parameters are non-negative. The parameters related to natural mortality at each life-stage and the environmental carrying capacity are positive and finite. Similarly the grouping and process for bounding from [29] and [19] is closely followed. The state variables are grouped by life-cycle stage, organism, and adult insecticide resistance status, let:

$$\begin{aligned} B_1 &= (S_H, E_H, I_H, R_H), \quad B_2 = (S_{ms}, E_{ms}, I_{ms}), \\ B_3 &= (S_{mr}, E_{mr}, I_{mr}), \quad B_4 = (E_m, L_m, P_m). \end{aligned}$$

Definition 1

Following [19], for the time-dependent parameters the following quantities are defined:

$$a^* = \sup_{t \geq 0} a(t), \quad a_* = \inf_{t \geq 0} a(t).$$

For the immature mosquito groups, since $(1 - (E/K_E))_+ \geq 0$, then $E(t) \leq K_E$ for all t . Thus, using Definition 1, it can be deduced from the immature mosquito compartments using the larval stage described in the model that

$$\dot{L} = \sigma_E(T)E - [\sigma_L(T) + \mu_L(T)]L \leq \sigma_E^* K_E - (\sigma_L^* + \mu_L^*)L,$$

so that following by the Gronwall inequality is

$$\limsup_{t \rightarrow \infty} L(t) \leq \frac{\sigma_E^* K_E}{\sigma_L^* + \mu_L^*} = L^\diamond.$$

With the bounds from above in the equations, it is similarly found that:

$$\limsup_{t \rightarrow \infty} P(t) \leq \frac{\sigma_L^* L^\diamond}{\sigma_P^* + \mu_P^*} = P^\diamond.$$

Let $N_{ms} = S_{ms} + E_{ms} + I_{ms}$ and $N_{mr} = S_{mr} + E_{mr} + I_{mr}$. Using the above equation, furthermore it can be shown for adult mosquito groups:

$$\dot{N}_{ms} = \sigma_P(T)(1-f)P - (\mu_{ms}(t) + \epsilon_B C_B \delta_B) N_{ms} \leq \sigma_P^*(1-f)P^\diamond - (\mu_{ms}^* + \epsilon_B C_B \delta_B) N_{ms},$$

from which it follows

$$\limsup_{t \rightarrow \infty} N_{ms}(t) \leq \frac{\sigma_P^*(1-f)P^\diamond}{\mu_{ms}^* + \epsilon_B C_B \delta_B} = N_{ms}^\diamond.$$

and similarly,

$$\limsup_{t \rightarrow \infty} N_{mr}(t) = \frac{\sigma_P^*(f)P^\diamond}{\mu_{mr}^* + \epsilon_B C_B \delta_B(1-u)} = N_{mr}^\diamond.$$

Lastly, the human compartment can be shown:

$$\dot{N}_H = \pi_H - \mu_H N_H(t) - \delta_H I_H(t) \leq \pi_H - \mu_H N_H(t).$$

It follows that $dN_H/dt < 0$ if $N_H(t) > \pi_H/\mu_H$. A standard comparison theorem can be used so that $N_H(t) \leq N_H(0)e^{-\mu_H t} + \frac{\pi_H}{\mu_H}[1 - e^{-\mu_H t}]$. Thus, $N_H \leq \pi_H/\mu_H$ if $N_H(0) \leq \pi_H/\mu_H$. Additionally, if $N_H(0) > \pi_H/\mu_H$, then $N_H(t) \rightarrow \pi_H/\mu_H$ as $t \rightarrow \infty$. That is,

$$\limsup_{t \rightarrow \infty} N_H(t) \leq \pi_H/\mu_H = N_H^\diamond.$$

Lemma 1. *All solutions of the model with non-negative initial values remain non-negative and bounded for all $t > 0$.*

Proof. The right side of the equations in the model are continuously differentiable and locally-Lipschitz at $t = 0$. From the Picard-Lindelöf theorem, it follows that a unique solution of the model with non-negative initial conditions exists in a region Ω for all $t > 0$. Since it was assumed that $(1 - \frac{E}{K_E})_+ \geq 0$ for all $t \geq 0$, then $E(t) \leq K_E$ for all $t \geq 0$. Therefore, $E(t) \leq K_E$ for all $t \geq 0$. From the other equations that follow, the solutions of the other state variables from the model are bounded and the solutions of the model are bounded. \square

Theorem 1. *The region $\Omega = \Omega_1 \times \Omega_2 \times \Omega_3 \times \Omega_4$ is positively-invariant and attracts all solutions of the model.*

Let

$$\begin{aligned} \Omega_1 &= \left(B_1 \in \mathbb{R}_+^4 : N_H(t) \leq \frac{\Pi_H}{\mu_H} \right), \\ \Omega_2 &= \left(B_2 \in \mathbb{R}_+^3 : N_{ms} \leq N_{ms}^\diamond \right), \\ \Omega_3 &= \left(B_3 \in \mathbb{R}_+^3 : N_{mr} \leq N_{mr}^\diamond \right), \\ \Omega_4 &= \left(B_4 \in \mathbb{R}_+^3 : E_m \leq K_E, L_m \leq L^\diamond, P_m \leq P^\diamond \right). \end{aligned}$$

Proof. This result follows from Lemma 1. The invariance of Ω_4 is established from if $E(t) > K_E$, then $\dot{E} < 0$. Also, $\dot{L} < 0$ when $L(t) > L^\diamond(t)$ and $\dot{P} < 0$ when $P(t) > P^\diamond(t)$. Similarly, for both Ω_2 and Ω_3 , $\dot{N}_{vs} < 0$ when $N_{vs}(t) > N_{vs}^\diamond(t)$ and $\dot{N}_{vr} < 0$ when $N_{vr}(t) > N_{vr}^\diamond(t)$. Lastly, for Ω_1 , $\dot{N}_H < 0$ when $N_H(t) > N_H^\diamond(t)$. Hence, the region $\Omega = \Omega_1 \times \Omega_2 \times \Omega_3 \times \Omega_4$ is positively invariant with respect to the model and attracts all positive solutions, since the sub-regions $\Omega_i (i = 1, 2, 3, 4)$ are positively-invariant and attracting with respect to the model, therefore it is sufficient to study the model within this range. \square

4.1.2 Existence and Asymptotic Stability of Equilibria

Here the dynamics of the autonomous version of the model are studied where weather-dependant parameters of the model are considered to be constants. It is convenient for the following entomological quantity to be identified, r_0 , which is the net production number which measures the average rate at which new adult female mosquitoes are produced. We begin with the following equation:

$$\begin{aligned} 0 = \dot{E} &= \eta_E(M^*) - \frac{\eta_E(E^*)(M^*)}{K_E} - K_1(E^*) \\ &= K_E \eta_E(M^*) - \frac{\eta_E(E^*)(M^*)K_E}{K_E} - K_1(E^*)K_E, \\ \implies E^* &= \frac{\eta_E(M^*)K_E}{K_E K_1 + \eta_E(M^*)}. \end{aligned}$$

Following the simplification for E^* , the following equations must be solved so that M^* may be substituted to solve for E^* . This is done by using subsequent equation solutions in the following order to write M^* in terms of E^* .

$$\begin{aligned} L^* &= \frac{\sigma_E(E^*)}{K_2}, \\ P^* &= \frac{\sigma_L(L^*)}{K_3} = \frac{\sigma_L \sigma_E(E^*)}{K_2 K_3}, \\ M^* &= \frac{q \sigma_P(P^*)}{K_4} = \frac{q \sigma_P \sigma_L \sigma_E(E^*)}{K_2 K_3 K_4}, \end{aligned}$$

where,

$$\begin{aligned} K_1 &= \sigma_E + \mu_E, K_2 = \sigma_L + \mu_L, \\ K_3 &= q \sigma_P + \mu_P, K_4 = \mu_{mr} + \epsilon_B C_B \delta_B (1 - u). \end{aligned}$$

Now E^* is solved with substitution giving:

$$E^* = \frac{\eta_E \left(\frac{q\sigma_P\sigma_L\sigma_E(E^*)}{K_2K_3K_4} \right) K_E}{K_1K_E + \eta_E \left(\frac{q\sigma_P\sigma_L\sigma_E(E^*)}{K_2K_3K_4} \right)},$$

$$K_1K_E + \frac{\eta_E q\sigma_P\sigma_L\sigma_E(E^*)}{K_2K_3K_4} = \frac{\eta_E q\sigma_P\sigma_L\sigma_E}{K_2K_3K_4} K_E,$$

$$K_1K_2K_3K_4K_E + \eta_E q\sigma_P\sigma_L\sigma_E(E^*) = \eta_E q\sigma_P\sigma_L\sigma_E K_E,$$

$$E^* = \frac{(\eta_E q\sigma_P\sigma_L\sigma_E - K_1K_2K_3K_4)K_E}{\eta_E q\sigma_P\sigma_L\sigma_E},$$

$$E^* = K_E \left(1 - \frac{K_1K_2K_3K_4}{\eta_E q\sigma_P\sigma_L\sigma_E} \right),$$

Hence,

$$r_0 = \frac{\eta_E q\sigma_P\sigma_L\sigma_E}{K_1K_2K_3K_4}.$$

Similarly to the method of inspection described by [29], r_0 can be determined as follows: it is the product of the rate at which the eggs are laid by adult female mosquitoes (η_E), the probability that the eggs survive and hatch into larvae ($\frac{\sigma_E}{K_1}$), the probability that the larvae survive and develop into pupae ($\frac{\sigma_L}{K_2}$), the probability that the pupae survive and mature into adult female mosquitoes ($\frac{q\sigma_P}{K_3}$), and the average lifespan of an adult female mosquito ($\frac{1}{K_4}$). The threshold quantity (r_0) is similar to the vectorial reproduction number, for which mosquito population exists whenever $r_0 > 1$ and no mosquito population exists for $r_0 < 1$ at equilibrium [30].

Now the asymptotic properties of different entomological states and disease presence are explored for understanding model behavior and related thresholds. The autonomous model has:

(i) A trivial disease free equilibrium (DFE) where no mosquitoes exist:

$$\mathcal{T}_1 = (S_H^*, E_H^*, I_H^*, R_H^*, S_{ms}^*, E_{ms}^*, I_{ms}^*, S_{mr}^*, E_{mr}^*, I_{mr}^*, E^*, L^*, P^*) = \left(\frac{\pi_H}{\mu_H}, 0, 0, 0, 0, 0, 0, 0, 0, 0, 0, 0, 0 \right).$$

(ii) A non-trivial sensitive-only disease-free boundary equilibrium:

$$\mathcal{T}_2 = (S_H^*, 0, 0, 0, S_{ms}^*, 0, 0, 0, 0, 0, E^*, L^*, P^*),$$

$$\text{where, } S_H^* = \frac{\pi_H}{\mu_H}, S_{ms}^* = \frac{\sigma_P(1-f)P^*}{\mu_{ms} + \epsilon_B C_B \delta_B}, E^* = K_E \left(1 - \frac{1}{r_0}\right), L^* = \frac{\sigma_L E^*}{\sigma_L + \mu_L}, \text{ and } P^* = \frac{\sigma_P L^*}{\sigma_P + \mu_P}.$$

(iii) A non-trivial resistant-only disease-free boundary equilibrium:

$$\mathcal{T}_3 = (S_H^{**}, 0, 0, 0, 0, 0, 0, S_{mr}^{**}, 0, 0, E^{**}, L^{**}, P^{**}),$$

$$\text{where, } S_H^{**} = \frac{\pi_H}{\mu_H}, S_{mr}^{**} = \mu_{mr} + \epsilon_B C_B \delta_B (1 - u), E^{**} = K_E \left(1 - \frac{1}{r_0}\right), L^{**} = \frac{\sigma_L E^{**}}{\sigma_L + \mu_L}, \text{ and } P^{**} = \frac{\sigma_P L^{**}}{\sigma_P + \mu_P}.$$

(iv) A non-trivial coexistence equilibrium which represents an equilibrium where the component of each state variable of the model is nonzero:

$$\mathcal{T}_4 = (S_H^{***}, E_H^{***}, I_H^{***}, R_H^{***}, S_{ms}^{***}, E_{ms}^{***}, I_{ms}^{***}, S_{mr}^{***}, E_{mr}^{***}, I_{mr}^{***}, E_H^{***}, L^{***}, P^{***}).$$

The next generation operator method can be used to analyze the local asymptotic stability of the DFE [31]. The associated matrix F (new infection terms) and matrix V (linear transition terms) are given, respectively, by:

$$F = \begin{bmatrix} 0 & 0 & 0 & 0 & 0 & \frac{\beta_{Hms} S_{ms}^*}{N_H^*} \\ 0 & 0 & 0 & 0 & 0 & 0 \\ 0 & 0 & 0 & 0 & 0 & \frac{\beta_{Hmr} S_{mr}^*}{N_H^*} \\ 0 & 0 & 0 & 0 & 0 & 0 \\ 0 & \frac{\beta_{msH} S_H^*}{N_H^*} & 0 & \frac{\beta_{mrH} S_H^*}{N_H^*} & 0 & 0 \\ 0 & 0 & 0 & 0 & 0 & 0 \end{bmatrix} \begin{bmatrix} E_{ms} \\ I_{ms} \\ E_{mr} \\ I_{mr} \\ E_H \\ I_H \end{bmatrix}$$

and,

$$V = \begin{bmatrix} \sigma_{ms} + \mu_{ms} & 0 & 0 & 0 & 0 & 0 \\ -\sigma_{ms} & \mu_{ms} & 0 & 0 & 0 & 0 \\ 0 & 0 & \sigma_{mr} + \mu_{mr} & 0 & 0 & 0 \\ 0 & 0 & -\sigma_{mr} & \mu_{mr} & 0 & 0 \\ 0 & 0 & 0 & 0 & \sigma_H + \mu_H & 0 \\ 0 & 0 & 0 & 0 & -\sigma_H & \gamma_H + \delta_H + \mu_H \end{bmatrix} \begin{bmatrix} E_{ms} \\ I_{ms} \\ E_{mr} \\ I_{mr} \\ E_H \\ I_H \end{bmatrix}.$$

The reproduction number (\mathcal{R}_0) of the model which considers the absence of all insecticide-based interventions, which in this model is only insecticide treated bed nets, is given by:

$$\mathcal{R}_0 = \rho(FV^{-1}),$$

which gives,

$$\begin{aligned}\mathcal{R}_0 &= \sqrt{\mathcal{R}_{0ms} + \mathcal{R}_{0mr}} \\ &= \sqrt{(\mathcal{R}_{0msH} \times \mathcal{R}_{0Hms}) + (\mathcal{R}_{0mrH} \times \mathcal{R}_{0Hmr})}.\end{aligned}$$

It is assumed in the model that the transmission rates between sensitive and resistant mosquito classes are equal where $\beta_{msH} = \beta_{mrH}$ and $\beta_{Hms} = \beta_{Hmr}$, thus are denoted as β_{mH} and β_{Hm} , respectively. Additionally, it is assumed in the model that the natural death rates and the developmental rates of sensitive and resistant mosquito classes are equal where $\mu_{mr} = \mu_{ms}$ and $\sigma_{mr} = \sigma_{ms}$ respectively, thus are denoted as μ_m and σ_m , respectively. Each of the constituent \mathcal{R} values at DFE are solved as,

$$\begin{aligned}\mathcal{R}_{msH} = \mathcal{R}_{mrH} &= \frac{\beta_{mH} S_H^* \sigma_H}{N_H^* (\sigma_H + \mu_H) (\gamma_H + \mu_H + \delta_H)}, \\ \mathcal{R}_{Hms} &= \frac{\beta_{Hm} S_{ms}^* \sigma_m}{N_H^* (\sigma_m + \mu_m) \mu_m}, \\ \mathcal{R}_{Hmr} &= \frac{\beta_{Hm} S_{mr}^* \sigma_m}{N_H^* (\sigma_m + \mu_m) \mu_m}.\end{aligned}$$

Also note for the DFE conditions,

$$\begin{aligned}S_{ms}^* &= \frac{\sigma_P (1-f) P^*}{\mu_m}, \\ S_{mr}^* &= \frac{\sigma_P (f) P^*}{\mu_m}.\end{aligned}$$

The value \mathcal{R}_C which is similar to \mathcal{R}_0 (although it also contains bed net coverage) is given as:

$$\mathcal{R}_C = \sqrt{(\mathcal{R}_{CmsH} \times \mathcal{R}_{CHms}) + (\mathcal{R}_{CmrH} \times \mathcal{R}_{CHmr})},$$

but now with each of the constituent \mathcal{R} values solved as,

$$\begin{aligned}\mathcal{R}_{msH} = \mathcal{R}_{mrH} &= \frac{(1 - \epsilon_B C_B) \beta_{mH} S_H^* \sigma_H}{N_H^* (\sigma_H + \mu_H) (\gamma_H + \mu_H + \delta_H)}, \\ \mathcal{R}_{Hms} &= \frac{\beta_{HM} S_{ms}^* \sigma_m}{N_H^* (\sigma_m + \mu_m + \epsilon_B C_B \delta_B) (\mu_m + \epsilon_B C_B \delta_B)}, \\ \mathcal{R}_{Hmr} &= \frac{\beta_{HM} S_{mr}^* \sigma_m}{N_H^* (\sigma_m + \mu_m + \epsilon_B C_B \delta_B) (\mu_m + \epsilon_B C_B \delta_B)}.\end{aligned}$$

where for the DFE conditions,

$$S_{ms}^* = \frac{\sigma_P (1 - f) P^*}{\mu_m + \epsilon_B C_B \delta_B}, \quad S_{mr}^* = \frac{\sigma_P (f) P^*}{\mu_m + \epsilon_B C_B \delta_B (1 - u)}.$$

The results below follow from Theorem 2 in [31].

Lemma 2: *The trivial disease free equilibrium is locally-asymptotically stable if $\mathcal{R}_0(\mathcal{R}_C) < 1$, and unstable if $\mathcal{R}_0(\mathcal{R}_C) > 1$.*

The \mathcal{R}_0 of the model is the geometric mean of the reproduction numbers for human-to-mosquito ($\mathcal{R}_{0,HM}$, $\mathcal{R}_{C,HM}$) and mosquito-to-human ($\mathcal{R}_{0,MH}$, $\mathcal{R}_{C,MH}$) transmission interactions. Due to two generations being required to complete the human-vector-human or vector-human-vector malaria transmission cycle, the geometric mean is present. The general epidemiological implication of this lemma is that a small influx of infected mosquitoes would not generate a large outbreak when \mathcal{R}_0 is less than unity and the disease would die out over time. Although, this may not always be the case due to backwards bifurcation as explored in [32].

As mentioned by [19], it can be shown using the next generation operator method that the associated reproduction number of the autonomous model is given by:

$$\mathcal{R}_{0ms} = \sqrt{\mathcal{R}_{Hms} \times \mathcal{R}_{msH}},$$

and

$$\mathcal{R}_{0mr} = \sqrt{\mathcal{R}_{Hmr} \times \mathcal{R}_{mrH}},$$

where separate calculations done by inspection for \mathcal{R}_{0ms} and \mathcal{R}_{0mr} shows, respectively:

$$\begin{aligned}\mathcal{R}_{msH} &= (1 - \epsilon_B C_B) \beta_{msH} \left(\frac{\sigma_H}{\sigma_H + \mu_H} \right) \left(\frac{1}{\gamma_H + \mu_H + \delta_H} \right), \\ \mathcal{R}_{Hms} &= \left(\frac{\beta_{HM} S_{ms}^*}{N_H^*} \right) \left(\frac{\sigma_{ms}}{\sigma_{ms} + \mu_{ms} + \epsilon_B C_B \delta_B} \right),\end{aligned}$$

and

$$\mathcal{R}_{mrH} = (1 - \epsilon_B C_B) \beta_{mrH} \left(\frac{\sigma_H}{\sigma_H + \mu_H} \right) \left(\frac{1}{\gamma_H + \mu_H + \delta_H} \right),$$

$$\mathcal{R}_{Hmr} = \left(\frac{\beta_{HM} S_{mr}^*}{N_H^*} \right) \left(\frac{\sigma_{mr}}{\sigma_{mr} + \mu_{mr} + \epsilon_B C_B \delta_B (1 - u)} \right),$$

thus giving the results:

$$\mathcal{R}_{0ms} = \sqrt{\frac{(1 - \epsilon_B C_B) \beta_{msH} \sigma_H \beta_{HM} S_{ms}^* \sigma_{ms}}{(\sigma_H + \mu_H)(\gamma_H + \mu_H + \delta_H) N_H^* (\sigma_{ms} + \mu_{ms} + \epsilon_B C_B \delta_B)}},$$

and

$$\mathcal{R}_{0mr} = \sqrt{\frac{(1 - \epsilon_B C_B) \beta_{mrH} \sigma_H \beta_{HM} S_{mr}^* \sigma_{mr}}{(\sigma_H + \mu_H)(\gamma_H + \mu_H + \delta_H) N_H^* [\sigma_{mr} + \mu_{mr} + \epsilon_B C_B \delta_B (1 - u)]}}.$$

Theorem 2: Relating to the competitive-exclusion principle, the sensitive-only (resistant-only) boundary equilibrium is locally-asymptotically stable if $\mathcal{R}_{0ms}(\mathcal{R}_{0mr}) > 1$ and $\mathcal{R}_{0mr}(\mathcal{R}_{0ms}) < 1$.

Conjecture 1: The model has a non-trivial coexistence equilibrium where all the states are nonzero and locally-asymptotically stable whenever $\min\{\mathcal{R}_{0ms}, \mathcal{R}_{0mr}\} \geq 1$.

4.2 Application results

As stated before, the application was primarily built using Python's backend framework Flask, and HTML/CSS and JavaScript in the frontend. The map shown to the user is generated using the Open Layers API in JavaScript. The code corresponding to the model was written in Python, and solved as a system of ordinary differential functions, using the *odeint* command from the *scipy* library. Data handling and API calls were done using Python as well.

Here is a how a normal user interaction would work. Every time a user clicked on the "Calculate Risk in my Area" button as shown in Figure 7, a request is sent to the backend along with the coordinates of the user's location. Several pieces of data are acquired, either locally stored or through third-party API calls, as discussed in Section 3.1. After acquiring this data, the model is solved using the *odeint* command and the entomological inoculation rate (EIR) is generated according to the equations mentioned previously. Recall that the equation for EIR as stated in section 2.5 is

$$EIR = \beta(1 - \epsilon_B C_B) \left(\frac{I_{ms} + I_{mr}}{N_H} \right).$$

After the model is solved as stated before, the final values of I_{ms} , I_{mr} , and N_H are taken and plugged into the EIR equation. Likewise, the value of β is calculated from the function defined in Table 4,

with ϵ_B and c_B sourced from APIs or locally saved datasets. This EIR value is then used to inform the relative risk of the user, which is shown to the user visually using the graph that is subsequently generated. The threshold for what should be considered high risk proved difficult to find during our research. An EIR value greater than 0.03 per day was chosen to be high risk in our MEWS, since it equates to around 10 infectious bites per year, but this value can and should be modified with further research.

There are several features of this application that makes it user-friendly and effective, as we have claimed. For starters, the application supports multiple African languages, including some of the most common ones, such as French, Swahili, Yoruba, and Igbo. It links several resources in the toggle bar to the left for the user to learn more about malaria, from reputable sources like the WHO. The application itself is extremely easy to use, with only needing the user to click the one button in the center of the screen. The results do not demand the user to be educated about malaria or compartmental models. It is shown in their local preferred language, as well as through the use of colors, as demonstrated in Figure 7. Additionally, the fact that this is available as both a website and mobile application ensures that the target audience is broadened, and the user is provided with the choice and convenience of using either. These features were included after we identified the shortcomings of some of the other MEWS that we stated in the Introduction.

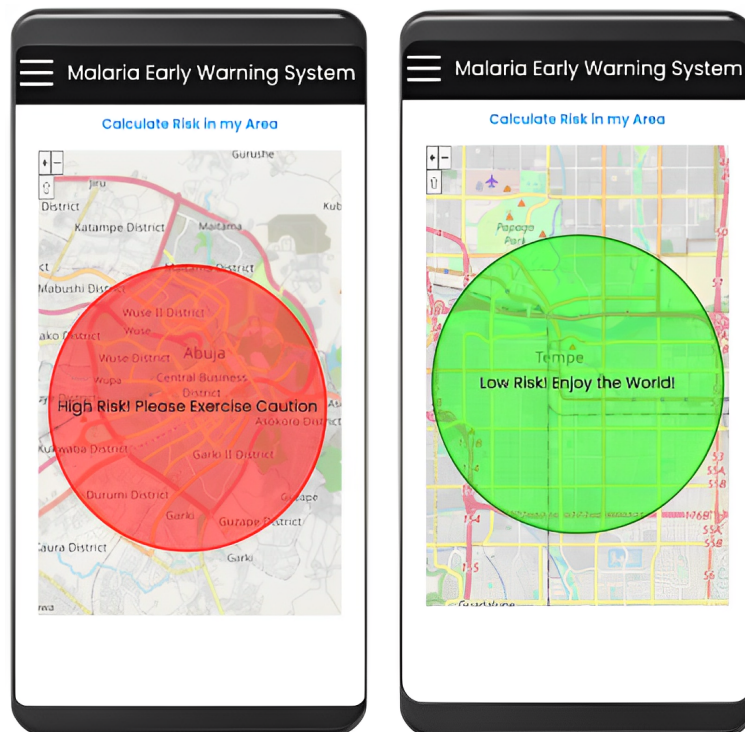


Figure 7. Sample outputs of the PWA based on different locations. The one on the left, where there is high risk, is the Nigerian city of Abuja. The right, where there is low risk, is Tempe, Arizona.

The above results correspond to the following model outputs in the backend. As can be seen, Tempe barely has any infection going around, as a result of it having historically low malaria prevalence and the lack of a high population of infected mosquitoes or humans, and so the EIR is essentially 0. However, there is a large number of infected mosquitoes and humans in Abuja, therefore leading to the warning shown to the user, with the EIR value for this city being around 0.4, meaning on average, a person will be bitten around 0.4 times by infectious mosquitoes *every day*. Although this may seem like a small number, it corresponds to around 150 infectious bites per year, meaning a person has relatively high risk of contracting malaria in this location. In extremely holoendemic areas, EIR values can go up to a whopping 500 per year. Please do note that the graphs are bound to change based on the initial starting conditions, which are included in Table 3 above.

For both locations in the plots below, the populations of mosquitoes show asymptotic behavior over time as it nears the carrying capacity. The susceptible human population decays at the death rate of humans, and specifically for Abuja, the infected human class recovers over time as well. However, this is where the difference in the level of risk of both locations come into picture. The population of susceptible humans falls drastically in Abuja; this is because, unlike Tempe where people are mostly dying of non-malaria related causes, people in Abuja are contracting and dying of malaria at higher numbers, leading to a huge drop in their population and consequently a high EIR value.

Malaria Model for Abuja, Nigeria

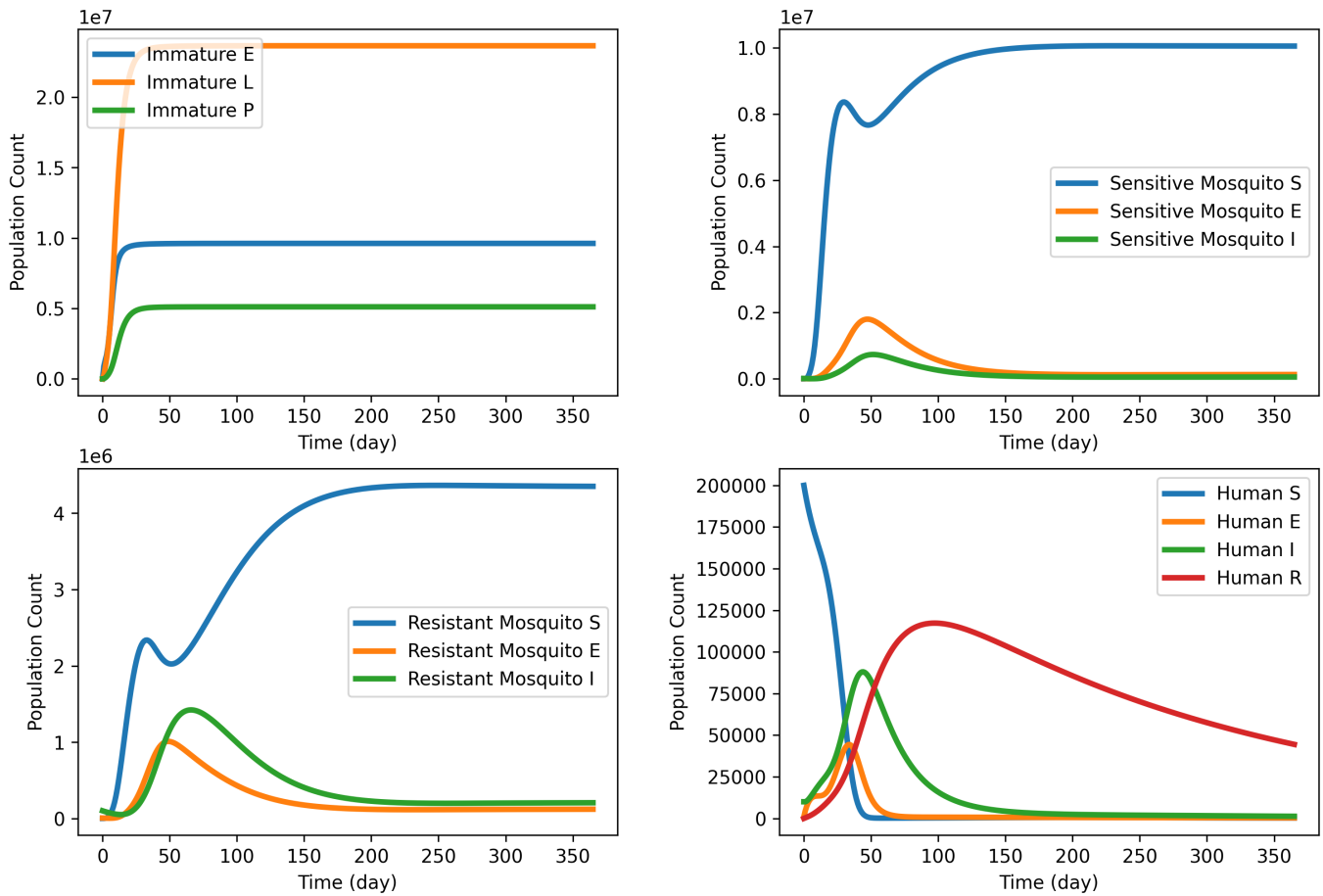


Figure 8. Output of the compartmental model for the city of Abuja, Nigeria. Top left corresponds to the Immature/Aquatic Mosquito Stage, top right to the Sensitive Adult Mosquito Stage, bottom left to the Resistant Adult Mosquito Stage, and bottom right to the Human dynamics. Please note the use of scientific notation in the plot axes of the top two and the bottom left graphs.

Malaria Model for Tempe, Arizona

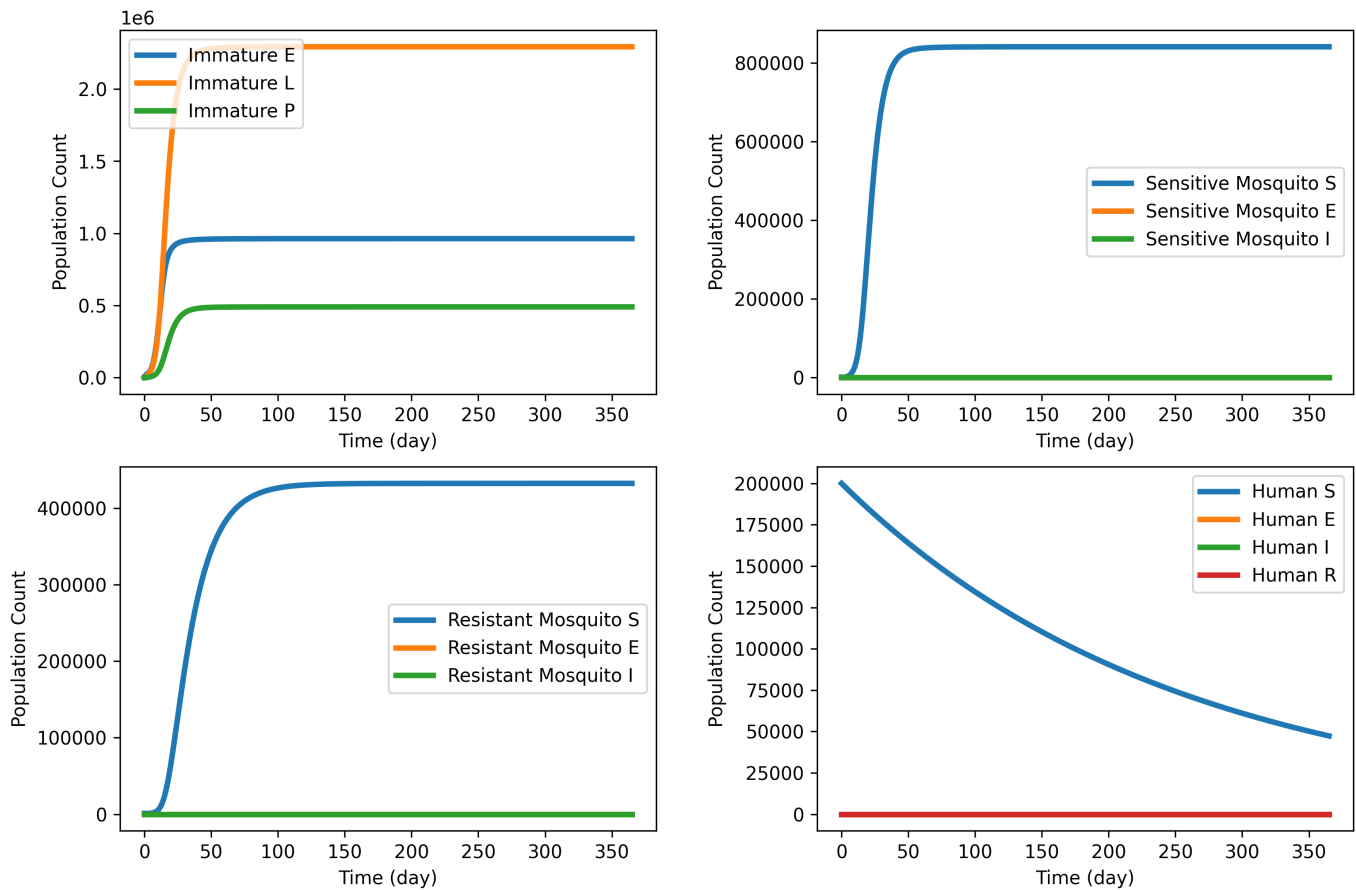


Figure 9. Output of the compartmental model for the city of Tempe, Arizona. Top left corresponds to the Immature/Aquatic Mosquito Stage, top right to the Sensitive Adult Mosquito Stage, bottom left to the Resistant Adult Mosquito Stage, and bottom right to the Human dynamics. Please note the use of scientific notation in the plot axes for the top left graph.

5. Discussion and Conclusion

We have presented a practical and important tool for preventing additional malaria cases through a web and mobile application. Used in combination with other preventive measures, such as LLINs and ITNs, the application will be highly effective in helping prevent new cases. Insecticide resistance is important to consider since it affects transmission rates, thus it is used in the application's mathematical model. Lastly, the application is user-friendly (simple to use and requires minimal interpretation from the user) and accessible to many (available in multiple languages).

In this study, adult mosquitoes and humans are given an SEI and SEIR model respectively in order to properly observe transmission. Both adult mosquitoes and humans are susceptible to

malaria. In addition, they both go through an exposed stage before becoming infectious. However, it is assumed that adult mosquitoes do not recover from malaria in contrast to humans. Bed net usage is also taken into consideration in the adult mosquito and human dynamics because it affects the rate of transmission.

Although immature mosquitoes cannot transmit malaria, they are an essential component in the math model. Without it, there could possibly be overestimation or underestimation of malaria burden [16]. As pupae mature into adults and adults reproduce to lay eggs, it is evident that immature and adult mosquitoes cannot be independently observed. The parameters in the immature stage are mostly temperature dependent, and since the adult dynamics is highly dependent on the immature stage and the human dynamics is highly dependent on adult mosquitoes, the overall model is dependent on the temperature. Temperature values for these parameters are obtained through a particular parameter in the immature dynamic, carrying capacity (K_E), which is dependent on precipitation since mosquitoes lay their eggs in bodies of water. The carrying capacity of eggs determines the maximum number of eggs to be laid in a particular region, which in turn determines the number of adult mosquitoes in that region. Therefore, carrying capacity has an indirect effect on the rate of transmission.

Using some values from the differential equations of the mosquito and human dynamics, the entomological inoculation rate (EIR) informs the risk of infection. That result is evaluated and then translated into a simple, user-friendly message, notifying the user of whether he or she is in a high or low risk region. Another way to determine risk is calculating the basic reproduction number (R_0). Ideally, EIR and R_0 would both be used as additional tools for determining an individual's risk. Unfortunately, due to its complexity, R_0 's results were impractical. Thus, only EIR was used to determine risk of infection.

The work presented in this paper provides a means of predicting an individual's risk of contracting malaria in a particular region. Such a prediction is vital in combating the spread of malaria because it can prevent an individual from traveling to a high-risk area, or it could encourage the individual to take protective measures, such as sleeping under a bed net or taking anti-malarial drugs before traveling. Using the differential equations in the mathematical model, we monitor possible transmission by calculating the number of immature mosquitoes, potential infectious adult mosquitoes, and infected humans in each region. The results from the differential equations provide the necessary values for calculating EIR, which will inform the user's risk. The intention is to format this early warning system as a mobile application and a website so the public can have access to it and stay informed.

The weather components including temperature and rainfall used in the model were integrated based on the previous work of other authors who fit parameters from fitting data sets with consideration of other models. Alternative models should also be taken into consideration such as the agent-based modeling approaches that emphasize weather effects on malaria incidence [33][34].

Although our dynamic MEWS is an important step forward in providing location and time-

specific malaria risk assessments to susceptible individuals, this study has several limitations. We could have worked with HydroSheds data to better inform the carrying capacity parameter for eggs in the aquatic stage. Furthermore, it is possible to obtain more granular weather data going back more than a year in the past. However, this requires a paid subscription. There are many such possibilities for improving upon the model we have used in this application, as well as the early warning system as a whole. Our main goal was to take the first step in creating an actual product by tackling some of the issues other MEWS presented, since to our knowledge, no one has attempted to do anything similar. We hope it will encourage others to adapt our model and build upon it, with the vision of eradicating malaria, or at the very least, act as a temporary remedial until an effective vaccine or better forms of combating malaria are discovered.

Acknowledgments

We would like to thank Dr. Fabio Milner, Director of the Simon A. Levin Mathematical, Computational and Modeling Sciences Center (Levin Center), for giving us the opportunity to participate in the Quantitative Research in the Life and Social Sciences program. We would also like to thank Co-Directors Dr. Abba Gumel and Dr. John Nagy for their efforts in planning and executing the program's instruction and activities. We also recognize the work of the many administrative staff and tutors who supported this effort. This research was conducted as part of 2022 QRLSSP at the Levin Center (MCMSC) at Arizona State University (ASU). This project has been partially supported by grants from the National Science Foundation (NSF Grant-DMS-1757968 and NSF Grant FAIN-2150492), the National Security Agency (NSA Grant H98230-20-1-0164), the Office of the President of ASU, and the Office of the Provost of ASU. We are especially grateful to Dr. Abba Gumel and Dr. Steffen Eikenberry for their guidance, as well as Hovig Artinian, Theophilus Kwofie, and Jordy Rodriguez for their support throughout the research.

References

- [1] Smith, M. L., & Styczynski, M. P. (2018). Systems Biology-Based Investigation of Host-Plasmodium Interactions. *Trends in parasitology*, 34(7), 617–632.
- [2] Max Roser and Hannah Ritchie (2019) - "Malaria". Published online at OurWorldInData.org. Retrieved from: <https://ourworldindata.org/malaria> [Online Resource]
- [3] Geneva: World Health Organization. (2021). World malaria report 2021. World Health Organization. <https://www.who.int/teams/global-malaria-programme/reports/world-malaria-report-2021>
- [4] Gallup, J., & Sachs, J. (2001). The economic burden of malaria, *The American Journal of Tropical Medicine and Hygiene* Am J Trop Med Hyg, 64(1_suppl). https://www.ajtmh.org/view/journals/tpmd/64/1_suppl/article-p85.xml

- [5] Centers for Disease Control and Prevention. (2021, December 16). CDC - Malaria - malaria worldwide - impact of malaria. Centers for Disease Control and Prevention. Retrieved from https://www.cdc.gov/malaria/malaria_worldwide/impact.html
- [6] Binka, F. N., Indome, F., & Smith, T. (1998). Impact of spatial distribution of permethrin-impregnated bed nets on child mortality in rural northern Ghana., *The American journal of tropical medicine and hygiene*, 59(1), 80-85. <https://www.ajtmh.org/view/journals/tpmd/59/1/article-p80.xml>
- [7] Eikenberry, S.E., Gumel, A.B. (2018). Mathematical modeling of climate change and malaria transmission dynamics: a historical review. *J. Math. Biol.* 77, 857–933. <https://doi.org/10.1007/s00285-018-1229-7>
- [8] Hemingway, J., Ranson, H., Magill, A., Kolaczinski, J., Fornadel, C., Gimnig, J., Coetzee, M., Simard, F., Roch, D. K., Hinzoumbe, C. K., Pickett, J., Schellenberg, D., Gething, P., Hoppé, M., & Hamon, N. (2016). Averting a malaria disaster: will insecticide resistance derail malaria control?. *Lancet* (London, England), 387(10029), 1785–1788. [https://doi.org/10.1016/S0140-6736\(15\)00417-1](https://doi.org/10.1016/S0140-6736(15)00417-1)
- [9] Grover-Kopec, E., Kawano, M., Klaver, R. W., Blumenthal, B., Ceccato, P., & Connor, S. J. (2005). An online operational rainfall-monitoring resource for epidemic malaria early warning systems in Africa. *Malaria Journal*, 4(1), 1-5. <https://link.springer.com/article/10.1186/1475-2875-4-6>
- [10] Malaria early warning system. Climate Data Library. (n.d.). Retrieved July 15, 2022, from <https://iridl.ldeo.columbia.edu/maproom/Health/Regional/Africa/Malaria/System.html>
- [11] Win Han Oo, Win Htike, Cutts, J.C. et al. A mobile phone application for malaria case-based reporting to advance malaria surveillance in Myanmar: a mixed methods evaluation. *Malar J* 20, 167 (2021). <https://doi.org/10.1186/s12936-021-03701-6>
- [12] Smith, D. L., Battle, K. E., Hay, S. I., Barker, C. M., Scott, T. W., & McKenzie, F. E. (2012). Ross, macdonald, and a theory for the dynamics and control of mosquito-transmitted pathogens. *PLoS pathogens*, 8(4), e1002588. <https://doi.org/10.1371/journal.ppat.1002588>
- [13] Lysenko, A., & Semashko, I. (1968). Geography of malaria. a medical-geographical study of an ancient disease. *Itogi Nauk Med Geogr.* Retrieved from <https://endmalaria.org/sites/default/files/lysenko.pdf>
- [14] Eikenberry, S.E., Gumel, A.B. (2019). Mathematics of Malaria and Climate Change. In: Kaper, H., Roberts, F. (eds) *Mathematics of Planet Earth. Mathematics of Planet Earth*, vol 5. Springer, Cham. https://doi.org/10.1007/978-3-030-22044-0_4
- [15] Centers for Disease Control and Prevention. (2022). Where malaria occurs. Centers for Disease Control and Prevention. <https://www.cdc.gov/malaria/about/distribution.html>
- [16] Agosto, F. B., Gumel, A. B., & Parham, P. E. (2015). Qualitative assessment of the role of temperature variations on malaria transmission dynamics. *Journal of Biological Systems*, 23(04), 1550030. <https://www.worldscientific.com/doi/abs/10.1142/s0218339015500308>

- [17] White, M. T., Griffin, J. T., Churcher, T. S., Ferguson, N. M., Basáñez, M. G., & Ghani, A. C. (2011). Modelling the impact of vector control interventions on *Anopheles gambiae* population dynamics. *Parasites & vectors*, 4(153). <https://doi.org/10.1186/1756-3305-4-153>
- [18] Mohammed-Awel, J., Iboi, E. A., & Gumel, A. B. (2020). Insecticide resistance and malaria control: A genetics-epidemiology modeling approach. *Mathematical biosciences*, 325, 108368. <https://doi.org/10.1016/j.mbs.2020.108368>
- [19] Kamaldeen Okuneye, Steffen E. Eikenberry & Abba B. Gumel. (2019). Weather-driven malaria transmission model with gonotrophic and sporogonic cycles. *Journal of Biological Dynamics*, 13, 288-324.
- [20] Mohammed-Awel, J., & Gumel, A. B. (2019). Mathematics of an epidemiology-genetics model for assessing the role of insecticides resistance on malaria transmission dynamics. *Mathematical Biosciences*, 312, 33-49. <https://www.sciencedirect-com.ezproxy1.lib.asu.edu/science/article/pii/S0025556417306636#fig0001>
- [21] Enahoro, I., Eikenberry, S., Gumel, A. B., Huijben, S., & Paaijmans, K. (2020). Long-lasting insecticidal nets and the quest for malaria eradication: a mathematical modeling approach. *Journal of Mathematical Biology*, 81(1), 113-158. <https://link.springer.com/article/10.1007/s00285-020-01503-z>
- [22] Beck-Johnson, L. M., Nelson, W. A., Paaijmans, K. P., Read, A. F., Thomas, M. B., & Bjørnstad, O. N. (2013). The effect of temperature on *Anopheles* mosquito population dynamics and the potential for malaria transmission. *PloS one*, 8(11).
- [23] Parham, P. E., & Michael, E. (2010). Modeling the effects of weather and climate change on malaria transmission. *Environmental health perspectives*, 118(5), 620–626. <https://doi.org/10.1289/ehp.0901256>
- [24] WorldClim. Maps, graphs, tables, and data of the global climate. 2022. <https://worldclim.org/>
- [25] WeatherAPI. JSON and XML Weather API and Geolocation Developer API. 2022. <https://www.weatherapi.com/>
- [26] Bhatt, S., Weiss, D. J., Cameron, E., Bisanzio, D., Mappin, B., Dalrymple, U., Battle, K., Moyes, C. L., Henry, A., Eckhoff, P. A., Wenger, E. A., Briët, O., Penny, M. A., Smith, T. A., Bennett, A., Yukich, J., Eisele, T. P., Griffin, J. T., Fergus, C. A., Lynch, M., ... Gething, P. W. (2015). The effect of malaria control on *Plasmodium falciparum* in Africa between 2000 and 2015. *Nature*, 526(7572), 207–211. <https://doi.org/10.1038/nature15535>
- [27] WorldPop Hub. Open and high-resolution geospatial data on population distributions, demographic and dynamics, with a focus on low and middle income countries. 2022. <https://hub.worldpop.org/doi/10.5258/SOTON/WP00004>
- [28] Malaria Atlas Project. International research collaboration that tracks malaria data primarily in Africa. 2022. <https://malariaatlas.org/>

- [29] Brozak, S. J., Mohammed-Awel, J., & Gumel, A. B. (2022). Mathematics of a single-locus model for assessing the impacts of pyrethroid resistance and temperature on population abundance of malaria mosquitoes. *Infectious Disease Modelling*, 7(3), 277–316. <https://doi.org/10.1016/j.idm.2022.05.007>
- [30] Okuneye, K., Abdelrazec, A., & Gumel, A. B. (2018). Mathematical analysis of a weather-driven model for the population ecology of mosquitoes. *Mathematical biosciences and engineering : MBE*, 15(1), 57–93. <https://doi.org/10.3934/mbe.2018003>
- [31] Van den Driessche, P., & Watmough, J. (2002). Reproduction numbers and sub-threshold endemic equilibria for compartmental models of disease transmission. *Mathematical biosciences*, 180(1-2), 29-48.
- [32] Garba, S. M., Gumel, A. B., & Abu Bakar, M. R. (2008). Backward bifurcations in dengue transmission dynamics. *Mathematical biosciences*, 215(1), 11–25. <https://doi.org/10.1016/j.mbs.2008.05.002>
- [33] Weidong Gu, Gerry F. Killeen, Charles M. Mbogo, James L. Regens, John I. Githure, & John C. Beier. (2003). An individual-based model of Plasmodium falciparum malaria transmission on the coast of Kenya, *Transactions of The Royal Society of Tropical Medicine and Hygiene*, 97(1), 43–50. [https://doi.org/10.1016/S0035-9203\(03\)90018-6](https://doi.org/10.1016/S0035-9203(03)90018-6)
- [34] Hoshen, M. B., & Morse, A. P. (2004). A weather-driven model of malaria transmission. *Malaria journal*, 3, 32. <https://doi.org/10.1186/1475-2875-3-32>